

# Tracking the dynamics of an ideal quantum measurement

Fabian Pokorny,<sup>1,\*</sup> Chi Zhang,<sup>1,†</sup> Gerard Higgins,<sup>1,‡</sup> Adán Cabello,<sup>2,§</sup> Matthias Kleinmann,<sup>3,4,¶</sup> and Markus Hennrich<sup>1,\*\*</sup>

<sup>1</sup>*Department of Physics, Stockholm University, 10691 Stockholm, Sweden*

<sup>2</sup>*Departamento de Física Aplicada II, Universidad de Sevilla, E-41012 Sevilla, Spain*

<sup>3</sup>*Department of Theoretical Physics, University of the Basque Country UPV/EHU, P.O. Box 644, E-48080 Bilbao, Spain*

<sup>4</sup>*Naturwissenschaftlich–Technische Fakultät, Universität Siegen, Walter-Flex-Straße 3, 57068 Siegen, Germany*

## Abstract

The existence of ideal quantum measurements is one of the fundamental predictions of quantum mechanics. In theory the measurement projects onto the eigenbasis of the measurement observable while preserving all coherences of degenerate eigenstates. The question arises whether there are dynamical processes in nature that correspond to such ideal quantum measurements. Here we address this question and present experimental results monitoring the dynamics of a naturally occurring measurement process: the coupling of a trapped ion qutrit to the photon environment. By taking tomographic snapshots during the detection process, we show with an average fidelity of 94% that the process develops in agreement with the model of an ideal quantum measurement.

---

\* [fabian.pokorny@fysik.su.se](mailto:fabian.pokorny@fysik.su.se)

† [chi.zhang@fysik.su.se](mailto:chi.zhang@fysik.su.se)

‡ [gerard.higgins@fysik.su.se](mailto:gerard.higgins@fysik.su.se)

§ [adan@us.es](mailto:adan@us.es)

¶ [matthias.kleinmann@uni-siegen.de](mailto:matthias.kleinmann@uni-siegen.de)

\*\* [markus.hennrich@fysik.su.se](mailto:markus.hennrich@fysik.su.se)

## I. INTRODUCTION

What is an ideal measurement in quantum mechanics? What are its inner workings? How does the quantum state change because of it? These have been central questions in the development of quantum mechanics [1]. Notably, today's accepted answer to the latter question is conceptually different from the one given in the first formalization of quantum mechanics by von Neumann [2]. Then, it was thought that an ideal measurement on a quantum system would inevitably destroy all quantum superpositions. Later, Lüders pointed out [3] that certain superpositions should survive, so that a sequence of ideal measurements would preserve quantum coherence. Lüders version is the one accepted today.

Even though there is agreement on the theoretical description of an ideal measurement, it is a fundamental question whether, and if so how, ideal measurements occur as natural processes. This is an especially sensitive question as measurements do not fall into the domain of unitary time evolution. In this Letter, we demonstrate a natural dynamical process that realizes an ideal quantum measurement. For this, we implement a natural process that is considered to be an ideal measurement, and monitor its dynamics by taking a sequence of snapshots while the process is occurring. These snapshots are tomographically complete and allow us to compare the experimental results with the theoretical prediction of an ideal measurement.

Ideal measurements model an ideal implementation of a quantum observable. In the discrete case, a measurement of the observable  $A$  yields values  $a_k$  according to the spectral decomposition  $A = \sum_k a_k \Pi_k$ , where  $\Pi_k$  are mutually orthogonal projections summing to identity, and  $a_k$  are distinct real numbers. Any measurement requires an interaction of the measurement apparatus with the system and this interaction affects the state of the system. This is true, independently of whether or not the measurement result is recorded by an observer. However, the effect on the state depends on the experimental realization. In practice, a measurement is often a rather violent process that “destroys” the quantum system, for example the detection of a photon.

A Lüders process is the ideal implementation of a measurement in which the state of the system is transformed according to [4]

$$\Xi_A: \rho \mapsto \sum_k \Pi_k \rho \Pi_k. \quad (1)$$

(For simplicity, we assume that the observer ignores the measurement outcome.) From a theoretical perspective, this process is truly special. On the one hand, it is the only process implementing a measurement of  $A$  which does not disturb any subsequent refined measurement  $B$  [5, 6]. That is, a measurement  $B$  where each

outcome  $\ell$  is at most as likely as a certain outcome  $k_\ell$  of  $A$ , for all states  $\rho$ . This implies that, whenever two observables  $A$  and  $B$  are compatible,  $AB = BA$ , then the respective Lüders processes do not disturb each other,  $\Xi_A \Xi_B = \Xi_B \Xi_A$  [3, 4]. On the other hand,  $\Xi_A$  is universal: any process  $\Lambda_A$  describing a measurement of  $A$  can be written as  $\Lambda_A: \rho \mapsto \sum_k \Phi_k(\Pi_k \rho \Pi_k)$ , where  $\Phi_k$  are some probability-preserving processes [4].

While these properties constitute strong theoretical arguments for the special role of the Lüders process, this does not imply that Lüders processes occur in nature. An important aspect of the Lüders process is that it leaves any quantum superposition of degenerate eigenstates unaffected. In this sense, the existence of Lüders processes is a nontrivial prediction of quantum mechanics that is usually taken for granted rather than tested thoroughly.

In order to investigate whether Lüders processes do exist in nature, we consider the canonical model for measurements [4, 7]: A system in state  $\rho$  is brought into contact with a pointer system, which is in state  $|\Phi\rangle$ . When in contact, the two systems interact via the Hamiltonian  $H_A$  for a time  $\tau$  and, after separating the two systems, the pointer system is measured in some fixed basis  $|\omega_j\rangle$ . This yields the process

$$M_A: \rho \mapsto \sum_j \langle \omega_j | e^{-iH_A \tau / \hbar} (\rho \otimes |\Phi\rangle\langle\Phi|) e^{iH_A \tau / \hbar} | \omega_j \rangle. \quad (2)$$

However, the class of processes covered by Eq. (2) is so general, that it can be shown [4] that any quantum process, including the Lüders processes  $\Xi_A$ , can be modeled by Eq. (2). Indeed, if we are able to engineer interactions and pointer systems at will as in, for example, quantum processors [8, 9], the fact that a process cannot be approximated by Eq. (2) would be in contradiction of our present understanding of those systems. Usually, experimental measurement procedures are not Lüders processes, because this would require a careful fine-tuning of the Hamiltonian  $H_A$  or else the degeneracy of the observable would be lifted by experimental imperfections which then leads to a process as the one envisioned by von Neumann, in which all coherences are destroyed.

## II. FLUORESCENCE MEASUREMENTS

The best candidate for a natural Lüders process is a interaction-free measurement, that is, a measurement of an observable of the form  $A = |\phi\rangle\langle\phi|$ , where the event “detection” corresponds to the eigenvalue 1 and the event “no detection” corresponds to the eigenvalue 0. There, it can be expected that the event “no detection” does not require any interaction with the eigenspace with eigenvalue

0 and hence superpositions in this subspace are preserved. Our choice for an experiment within which to identify a Lüders process is the coupling of a single trapped ion to the photon environment. To explain why this is a good candidate, it is useful to present a simplified description of the specific physical process in our experiment. For a more accurate theoretical model of this process see Ref. [10] and the Appendix.

We prepare an ion in a superposition of three electronic states,  $|0\rangle$ ,  $|1\rangle$ , and  $|2\rangle$ . By driving the transition  $|0\rangle$  to a short-lived excited level  $|e\rangle$ , we facilitate the emission of photons into the environment, via the natural decay  $|e\rangle |n=0\rangle \rightarrow |0\rangle |n=1\rangle$ . Here,  $|n=0\rangle$  is the initial state of the photon environment and  $|n=1\rangle$  the state of the photon environment after a photon has been emitted by the decay. We write the initial state of the system and the photon environment as

$$|\Psi\rangle = (\alpha_0 |0\rangle + \alpha_1 |1\rangle + \alpha_2 |2\rangle) |n=0\rangle. \quad (3)$$

Since only the level  $|0\rangle$  participates in the driving  $|0\rangle \leftrightarrow |e\rangle$  and the subsequent decay, the state after the driving is

$$|\Psi_m\rangle = \alpha_0 |0\rangle (g_0 |n=0\rangle + g_1 |n=1\rangle) + (\alpha_1 |1\rangle + \alpha_2 |2\rangle) |n=0\rangle, \quad (4)$$

where  $g_1$  is related to the probability of photon scattering by  $P_{\text{scatt}} = |g_1|^2$ , and  $|g_0|^2 + |g_1|^2 = 1$ . Ignoring the photon environment, we obtain the reduced state

$$\rho_m = \begin{pmatrix} |\alpha_0|^2 & \alpha_0 \alpha_1^* g_0 & \alpha_0 \alpha_2^* g_0 \\ \alpha_0^* \alpha_1 g_0^* & |\alpha_1|^2 & \alpha_1 \alpha_2^* \\ \alpha_0^* \alpha_2 g_0^* & \alpha_1^* \alpha_2 & |\alpha_2|^2 \end{pmatrix}. \quad (5)$$

The coherence between the levels  $|1\rangle$  and  $|2\rangle$  is preserved while the coherences between  $|0\rangle$  and  $|1\rangle$  and between  $|0\rangle$  and  $|2\rangle$  decay with  $|g_0|$ .

Intuitively, if at least one photon is scattered into the environment, then  $|g_0| = 0$  and the coupling to the photon environment corresponds to the measurement of the qutrit projection  $|0\rangle\langle 0|$ . Because the probability for scattering is  $P_{\text{scatt}} = 1 - |g_0|^2$  the implemented measurement is the generalized measurement  $(E_1, E_0)$  with  $E_1 = P_{\text{scatt}} |0\rangle\langle 0|$  and  $E_0 = \mathbb{1} - E_1$ . The numerical value of  $g_0$  depends on the experimental configuration and its computation requires a more rigorous model of the measurement process. A formula for  $g_0$  is given in Eq. (7) below and  $P_{\text{scatt}}$  is varied between 0.33 and 1.0, see Fig. 2.

Since our computation of the state  $\rho_m$  is generic for any initial state, we can read off the measurement process  $\Lambda_m$  as

$$\Lambda_m: \rho \mapsto \sqrt{E_1} \rho \sqrt{E_1} + G \sqrt{E_0} \rho \sqrt{E_0} G^\dagger, \quad (6)$$

with  $G = e^{i\varphi}|0\rangle\langle 0| + |1\rangle\langle 1| + |2\rangle\langle 2|$  and  $\varphi = \arg(g_0)$ . For  $P_{\text{scatt}} \rightarrow 1$ , this process implements the Lüders process  $\Xi_A$  for the observable  $A = |0\rangle\langle 0|$  and hence constitutes an ideal measurement. For  $P_{\text{scatt}} < 1$ , the process is a transitional form between  $\Xi_A$  and the trivial process  $\rho \mapsto \rho$ . Then, not only are the coherence between  $|1\rangle$  and  $|2\rangle$  preserved but also partially the coherences between  $|0\rangle$  and the other two qutrit levels. The occurrence of the terms  $\sqrt{E_k}\rho\sqrt{E_k}$  in  $\Lambda_m$  is in accordance to the canonical form of such transitional processes [4], while the phase  $e^{i\varphi}$  introduced by the unitary  $G$  is specific to this measurement process.

### III. EXPERIMENTAL SETUP

Our setup consists of a single  $^{88}\text{Sr}^+$  ion confined in a linear Paul trap, similar to Ref. [11]. Fig. 1 (a) shows the level scheme of the ion with the qutrit states encoded in electronic states of the ion. The measurement process is implemented using a pulse of 422 nm laser light, which facilitates coupling of the electronic state  $|0\rangle$  and the photon environment, while the qutrit levels  $|1\rangle$  and  $|2\rangle$  are left unaffected. We use the same laser light during the fluorescence detection step.

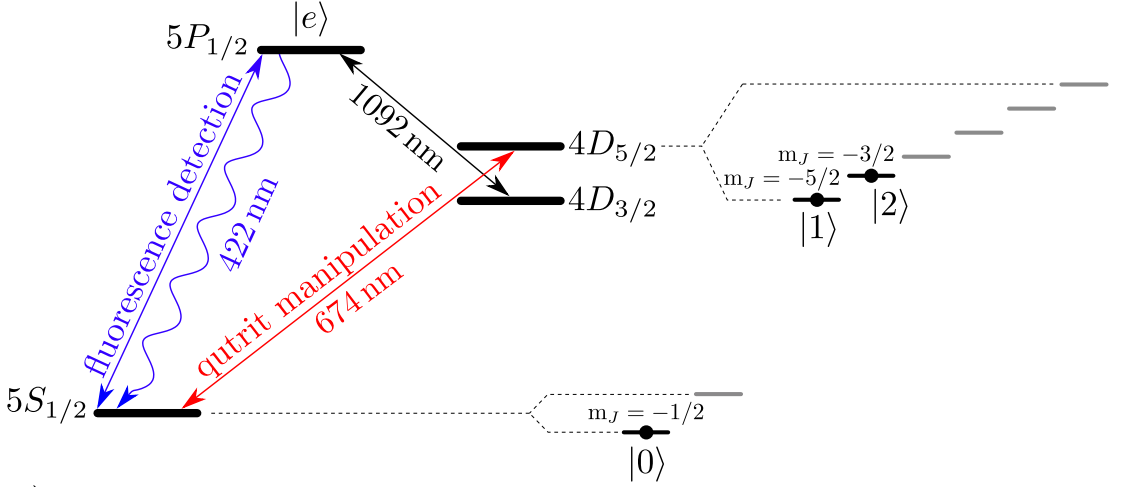
The variable  $g_0$  is obtained from a quantum optical model of the measurement, see Appendix. This yields

$$g_0 \approx \exp\left(-\frac{\Omega^2}{2\Gamma + 4i\Delta}t\right) \cdot \exp(i\phi_r), \quad (7)$$

where  $\Omega$  is the Rabi frequency driving the  $|0\rangle \leftrightarrow |e\rangle$  transition,  $\Gamma = 2\pi \times 21.65 \text{ MHz}$  [12] is the decay rate of state  $|e\rangle$ ,  $\Delta = 2\pi \times (5 \pm 2) \text{ MHz}$  the detuning from resonance,  $t = 1 \text{ ns}$  is the length of the laser pulse and the phase  $\phi_r$  results from the ac-Stark shifts induced by repump laser fields at 422 nm and 1092 nm which are present during the measurement process. The intensities and detunings of the repump fields are tuned such that  $\text{Im}(g_0) \approx 0$ . Values of  $\Omega$  and  $\Delta$  are determined from the  $5S_{1/2} \leftrightarrow 5P_{1/2}$  spectral lineshape.

We track the dynamics of the measurement process by carrying out process tomography as the power of the 422 nm laser used for coupling  $|0\rangle \leftrightarrow |e\rangle$  is varied. For the process tomography [Fig. 1 (b)], the ion is prepared in  $|0\rangle$ , then rotated (unitary  $U_i$ ) to one of the nine initial states  $|\psi_i\rangle$  using pulses of 674 nm laser light, see Table II in the Appendix. Then the measurement process is carried out; a 422 nm laser pulse is applied for 1 ns. Finally the state tomography is carried out by applying rotation  $U_j^\dagger$  followed by fluorescence detection for 500 ns. The measurement process uses a shorter pulse length than the fluorescence detection step, since the photons scattered during the measurement process do not need to be detected. During state tomography the rotation  $U_j^\dagger$  followed by a measurement of

a)



b)

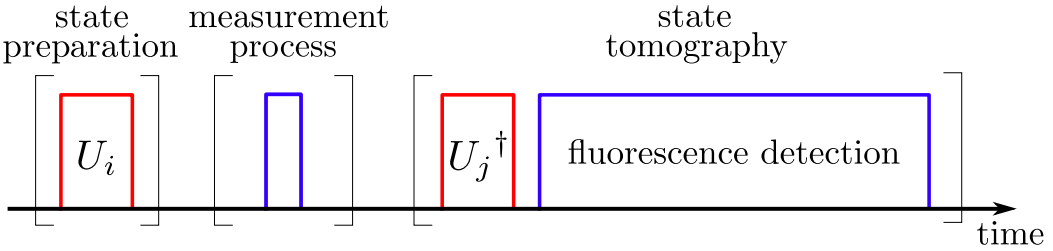


FIG. 1. Experimental realization of the process tomography of a Lüders measurement. (a) Level scheme of  $^{88}\text{Sr}^+$ . A magnetic field of  $(0.3576 \pm 0.0009)$  mT applied along the trap axis splits the  $m_J = -5/2$  and  $m_J = -3/2$  Zeeman sublevels of the metastable states  $4D_{5/2}$  by  $2\pi \times 6.0$  MHz. Together with the  $5S_{1/2}$   $m_J = -1/2$  ground state, these states form the qutrit basis states  $|0\rangle$ ,  $|1\rangle$ , and  $|2\rangle$ . The qutrit transitions are driven by a narrow-linewidth laser at 674 nm (linewidth  $< 2\pi \times 600$  Hz) tuned to either the  $|0\rangle \leftrightarrow |1\rangle$  or  $|0\rangle \leftrightarrow |2\rangle$  transition. A 422 nm laser driving the  $|0\rangle \leftrightarrow |e\rangle \equiv 5P_{1/2}$  transition is used to induce the Lüders measurement process and the fluorescence detection during state tomography. To prevent loss of population from the qutrit subspace during the measurement process 1092 nm laser light and circularly-polarised 422 nm laser light is used to repump population from  $4D_{3/2}$  and  $5S_{1/2}$   $m_J = +1/2$  to  $|0\rangle$ . (b) Experimental sequence for the process tomography. First the ion is prepared in one of nine initial states (Appendix, Table II) followed by a measurement which implements snapshots of an ideal measurement process and finally state tomography is performed using a qutrit rotation and fluorescence detection.

$(|0\rangle\langle 0|, \mathbb{1} - |0\rangle\langle 0|)$  acts as measurement operator  $(|\psi_j\rangle\langle\psi_j|, \mathbb{1} - |\psi_j\rangle\langle\psi_j|)$ . The nine initial states are each measured by the nine different operators; this is sufficient to characterize the experimental process.

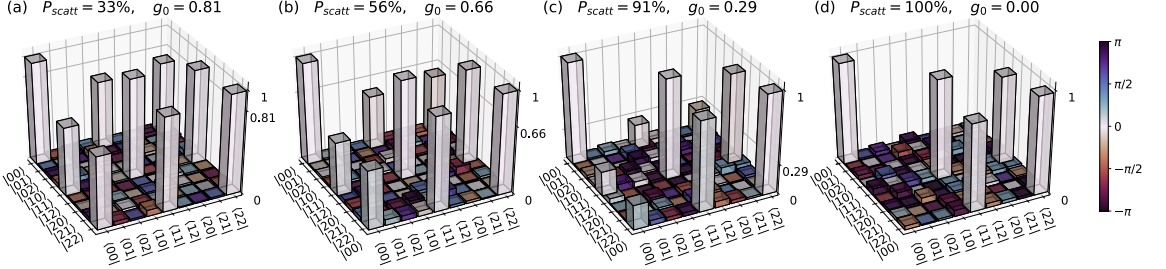


FIG. 2. Choi matrices  $\chi_{\text{exp}}$  reconstructed from the experimental data. The colors indicate the complex phase,  $g_0$  is calculated according to our model, see Eq. (7). From (a) to (d) the coupling strength of  $|0\rangle$  to the photon environment is increased and coherences involving state  $|0\rangle$  are destroyed. (d) is similar to the ideal Lüders process, and from (d)  $\rightarrow$  (a) the process becomes more similar to the trivial process  $\rho \mapsto \rho$ .

#### IV. RESULTS

For analyzing the experiment, a process  $\Lambda$  is more conveniently represented by its Choi matrix [4],

$$\chi = \sum_{i,j=0}^2 \Lambda[|i\rangle\langle j|_{\text{sys}}] \otimes |i\rangle\langle j|_{\text{aux}}. \quad (8)$$

This matrix is positive semidefinite for any physical process and yields a complete characterization of  $\Lambda$ , since  $\Lambda[\rho] = \text{tr}_{\text{aux}}[\chi(\mathbb{1} \otimes \rho^T)]$  with  $\rho^T = \sum_{i,j} |i\rangle\langle j| \langle j|\rho|i\rangle$ . If  $\Lambda$  is a probability-preserving process, that is,  $\text{tr}(\Lambda[\rho]) = \text{tr}(\rho) = 1$ , then the Choi matrix obeys  $\text{tr}_{\text{sys}}(\chi) = \mathbb{1}_{\text{aux}}$ . For the measurement process  $\Lambda_m$  in this work, the Choi matrix reads

$$\chi_m = |00\rangle\langle 00| + |\xi\rangle\langle\xi| + g_0|00\rangle\langle\xi| + g_0^*|\xi\rangle\langle 00|, \quad (9)$$

where  $|\xi\rangle = |11\rangle + |22\rangle$ .

The system is prepared in  $|\psi_i\rangle$ , the process  $\Lambda_m$  is carried out and subsequently the system is measured using the observable  $|\psi_j\rangle\langle\psi_j|$ . This is repeated  $N = 1000$  times for each  $i, j$ , with measurement outcome 1 occurring  $n_{i,j}$  times, and thus resulting in the experimental outcome frequency  $f_{i,j} = n_{i,j}/N$ . We use  $f_{i,j}$  to

reconstruct the experimental Choi matrix  $\chi_{\text{exp}}$  with  $\chi_{\text{exp}} = \arg \min_{\chi} \sum_{i,j} (p_{i,j} - f_{i,j})^2$  where the probabilities  $p_{i,j}$  are given by

$$\begin{aligned} p_{i,j} &= \langle \psi_j | \Lambda[|\psi_i\rangle\langle\psi_i|] | \psi_j \rangle \\ &= \text{tr}[\chi |\psi_j\rangle\langle\psi_j| \otimes |\psi_i\rangle\langle\psi_i|^T]. \end{aligned} \quad (10)$$

In addition we calculate the Uhlmann fidelity (rescaled by  $\frac{1}{9}$ ) of the experimental Choi matrix and the model to be on average 94%. For details see the Appendix.

$\chi_{\text{exp}}$  does not perfectly obey the probability-preserving constraint  $\text{tr}_{\text{sys}} \chi = \mathbb{1}_{\text{aux}}$ , due to statistical fluctuations and imperfections in the experimental setup. A likelihood ratio test shows that the deviation from  $\text{tr}_{\text{sys}} \chi = \mathbb{1}_{\text{aux}}$  is statistically significant by between 4 and 8 standard deviations. This can be attributed to imperfect state preparation. While the effect is statistically significant, it is clear from the high number of samples that the systematic deviation is overall very small and can be neglected. In the Appendix (Fig. C) we show a comparison of the  $\chi_{\text{exp}}$  reconstructed from experimental data with our model predictions including the respective uncertainties. We also show post-process density matrices for the initial state  $\frac{1}{\sqrt{2}} (|1\rangle + i|2\rangle)$  – the coherence is preserved, and for the initial state  $\frac{1}{\sqrt{2}} (|0\rangle + i|2\rangle)$  – the coherence is destroyed.

## V. CONCLUSION

Fluorescence detection is the standard way to measure a qubit in an ion trap or in similar setups that enable quantum information processing. This process is a prime example of an ideal measurement process: The system which is subject to the measurement is brought into contact with a macroscopic pointer state by facilitating a strong interaction between the system and the photon environment. A measurement of the photon environment then reveals the measurement outcome. Hence the measurement should behave as predicted by quantum mechanics for ideal measurements, that is, any coherence between all levels that are not measured should persist. We verified this property by performing process tomography of the coupling of an electronic state of a single trapped ion to the photon environment. The fidelity between the ideal measurement process and our implementation is 94% and matches the quality of a similar experiment [13] in a superconducting quantum system.

The theoretically ideal measurement process only occurs in the case of a strong interaction. If the interaction is weakened, then an intermediate process between the ideal measurement process and the identity process occurs. In the mathematical theory of measurements [4], such ideal measurements have a canonical



“square root” form, see Eq. (6). The quantum optical model for a weak measurement predicts a similar form which is only different in an additional phase between  $|0\rangle$  and the other levels. In process tomographies for those intermediate processes we obtain an overall process fidelity with the predicted model of approximately 94%.

We thus quantitatively demonstrated how a measurement can be implemented while preserving coherence and in which sense nature allows us to implement a weak measurement. A future direction of research is to test the predictions of ideal quantum measurements beyond what we have tested here: In the current experiment, the coherence-preserving measurement works relatively effortless, since the measurement process only affects a single state of our qutrit. This corresponds to a interaction-free measurement where it is only measured whether or not the system is in state  $|0\rangle$ . It could also be possible to find an ideal measurement process in nature, where all eigenvalues of the measured observable are two-fold degenerate and therefore the coherence between the degenerate eigenstates needs to be preserved. Whether such processes exist as natural processes and can be implemented with a fidelity comparable to our experiment is an open question.

## VI. ACKNOWLEDGEMENTS

We thank Mohamed Bourennane and Markus Müller for discussions. This work was supported by the Spanish Ministry of Economy, Industry and Competitiveness MINECO and the European Regional Development Fund FEDER through Grant No. FIS2017-89609-P and No. FIS2015-67161-P, by the FQXi Large Grant “The Observer Observed: A Bayesian Route to the Reconstruction of Quantum Theory,” by the EU (ERC Consolidator Grant No. 683107/TempoQ and ERC Starting Grant No. 258647/GEDENTQOPT), by the Basque Government (Grant No. IT986-16), by the Swedish Research Council (Trapped Rydberg Ion Quantum Simulator), by QuantERA project “ERyQSenS”, and by the project “Photonic Quantum Information” (Knut and Alice Wallenberg Foundation, Sweden).

- 
- [1] J. A. Wheeler and W. H. Zurek (eds.), *Quantum Theory and Measurement* (Princeton University Press, Princeton, NJ, 1983).
  - [2] J. von Neumann, *Mathematische Grundlagen der Quantenmechanik* (Springer-Verlag, Berlin, 1932) [*Mathematical Foundations of Quantum Mechanics* (Princeton University Press, Princeton, NJ, 1955)], in particular Chapter 5, Section 1.

- [3] G. Lüders, Über die Zustandsänderung durch den Meßprozeß, *Ann. Phys. (Leipzig)* **443**, 322 (1951) [Concerning the state-change due to the measurement process, *Ann. Phys. (Leipzig)* **15**, 663 (2006)].
- [4] T. Heinosaari and M. Ziman, *The Mathematical Language of Quantum Theory: From Uncertainty to Entanglement* (Cambridge University Press, Cambridge, UK, 2012).
- [5] G. Chiribella and X. Yuan, Measurement sharpness cuts nonlocality and contextuality in every physical theory arXiv:1404.3348.
- [6] M. Kleinmann, Sequences of projective measurements in generalized probabilistic models *J. Phys. A: Math. Theor.* **47**, 455304 (2014).
- [7] A. Peres, *Quantum Theory: Concepts and Methods* Kluwer (Kluwer, Dordrecht, 1995).
- [8] A. Barenco, C. H. Bennett, R. Cleve, D. P. DiVincenzo, N. Margolus, P. Shor, T. Sleator, J. A. Smolin, H. Weinfurter, Elementary gates for quantum computation, *Phys. Rev. A*, **52**, 3457 (1995).
- [9] D. Deutsch, Quantum theory, the Church–Turing principle and the universal quantum computer, *Proc. Roy. Soc. A*, **400**, 97–117 (1985).
- [10] H. Carmichael, *An Open Systems Approach to Quantum Optics* (Springer-Verlag, Berlin, 1993)
- [11] G. Higgins, W. Li, F. Pokorny, C. Zhang, F. Kress, C. Maier, J. Haag, Q. Bodart, I. Lesanovsky, and M. Hennrich, Single Strontium Rydberg Ion Confined in a Paul Trap, *Phys. Rev. X* **7**, 021038 (2017).
- [12] A. Gallagher, Oscillator Strengths of Ca II, Sr II, and Ba II, *Phys. Rev.* **157**, 24 (1967).
- [13] M. Jerger, P. Macha, A. R. Hamann, Y. Reshitnyk, K. Juliusson, and A. Fedorov, Realization of a Binary-Outcome Projection Measurement of a Three-Level Superconducting Quantum System *Phys. Rev. Applied*, **6**, 6, 014014 (2016).

## Appendix A: Appendix: Model for measurement process

We consider the transition between a ground state  $|0\rangle$  and a short-lived excited state  $|e\rangle$  of the trapped ion. This transition is driven with Rabi frequency  $\Omega$  using a classical laser field, where the laser frequency is detuned from resonance by  $\Delta$ . In the rotating-wave approximation, the interaction Hamiltonian is then given by [10]

$$H_I = \hbar\Delta|e\rangle\langle e| + \frac{\hbar\Omega}{2}(\sigma_+ + \sigma_-), \quad (\text{A1})$$

written in the frame rotating with the laser field. Here,  $\sigma_+ = |e\rangle\langle 0| = \sigma_-^\dagger$ . The other levels used in our system,  $|1\rangle$  and  $|2\rangle$ , are unaffected by the driving laser, so that  $H_I$  does not have contributions involving those levels.

The excited state decays back to the ground state with decay rate  $\Gamma$  and on decay, a photon is emitted into the photonic environment. In the Born–Markov approximation, this environment can be traced out and the state  $\rho$  of the levels  $|0\rangle$ ,  $|1\rangle$ ,  $|2\rangle$ , and  $|e\rangle$  follows a master equation in Lindblad form [10]. In the interaction

picture, this equation reads

$$\dot{\rho} = -\frac{i}{\hbar}[H_I, \rho] + \frac{\Gamma}{2}(2\sigma_- \rho \sigma_+ - \sigma_+ \sigma_- \rho - \rho \sigma_+ \sigma_-). \quad (\text{A2})$$

Without the laser ( $\Omega = 0$ ) we have  $\dot{\rho}_{e,e} = -\Gamma \rho_{e,e}$  and hence after a very short time ( $\sim \Gamma^{-1}$ ) the excited state relaxes,  $\rho_{e,e} = 0$ . Since we assume that there was no population of the excited level in the initial state, it is sufficient to consider the qutrit part of  $\rho$ . The transformation  $\Lambda_m$  induced by the measurement is then

$$\Lambda_m[\rho] = \begin{pmatrix} \rho_{0,0} & \rho_{0,1} g_0 & \rho_{0,2} g_0 \\ \rho_{1,0} g_0^* & \rho_{1,1} & \rho_{1,2} \\ \rho_{2,0} g_0^* & \rho_{2,1} & \rho_{2,2} \end{pmatrix}, \quad (\text{A3})$$

in accordance with Eq. (6). The variable  $g_0 \equiv g_0(t)$  is determined by the solution of the master equation (A2) for  $\rho_{0,1}$ , namely,

$$\dot{\rho}_{0,1} = -i\frac{\Omega}{2}\rho_{e,1}, \quad (\text{A4})$$

$$\dot{\rho}_{e,1} = -i\frac{\Omega}{2}\rho_{0,1} - \left(\frac{\Gamma}{2} + i\Delta\right)\rho_{e,1}. \quad (\text{A5})$$

These equations can be solved exactly, but yield impractical expressions. However, for  $\Omega \ll \Gamma$  the excited state can be adiabatically eliminated via  $\dot{\rho}_{e,1} \approx 0$ . With this approximation, Eq. (7) follows at once.

## Appendix B: Appendix: Experimental settings

	Power [W]	$\Omega$ [ $2\pi$ MHz]	$P_{\text{scatt}}$	$F$
(a)	0.08	$1.3 \pm 0.1$	$(33^{+7}_{-6})\%$	0.94
(b)	0.16	$1.9 \pm 0.2$	$(56^{+8}_{-9})\%$	0.95
(c)	0.48	$3.2 \pm 0.3$	$(91^{+4}_{-6})\%$	0.93
(d)	10.75	$15.2 \pm 1.5$	100%	0.94

TABLE I. Experimental settings: power of the laser used to drive the  $|0\rangle \leftrightarrow |e\rangle$  transition measured directly before the experiment chamber, corresponding Rabi frequency  $\Omega$ , photon scattering probability  $P_{\text{scatt}} = 1 - |g_0|^2$ , and experimental process fidelity  $F$  with the model process  $\Lambda_m$ . The statistical uncertainty of  $F$  is  $\pm 0.01$ .

The fidelity  $F$  between the experimental process and the model process  $\Lambda_m$  is given by

$$F = \frac{1}{9} \left[ \text{tr} \left( \sqrt{\sqrt{\chi_m} \chi_{\text{exp}} \sqrt{\chi_m}} \right) \right]^2, \quad (\text{B1})$$

with model Choi matrix  $\chi_m$  and experimental Choi matrix  $\chi_{\text{exp}}$ .

### Appendix C: Appendix: Initial state preparation

$j$	$U_j$	$ \psi_j\rangle = U_j  0\rangle$
1	$\mathbb{1}$	$ 0\rangle$
2	$R_y^1(\pi)$	$ 1\rangle$
3	$R_y^2(\pi)$	$ 2\rangle$
4	$R_y^1(\pi/2)$	$\frac{1}{\sqrt{2}}( 0\rangle +  1\rangle)$
5	$R_{-x}^1(\pi/2)$	$\frac{1}{\sqrt{2}}( 0\rangle + i 1\rangle)$
6	$R_y^2(\pi/2)$	$\frac{1}{\sqrt{2}}( 0\rangle +  2\rangle)$
7	$R_{-x}^2(\pi/2)$	$\frac{1}{\sqrt{2}}( 0\rangle + i 2\rangle)$
8	$R_y^2(\pi)R_y^1(\pi/2)$	$\frac{1}{\sqrt{2}}( 1\rangle +  2\rangle)$
9	$R_y^2(\pi)R_{-x}^1(\pi/2)$	$\frac{1}{\sqrt{2}}( 1\rangle + i 2\rangle)$

TABLE II. Pulse sequences for the implementation of the unitaries  $U_j$ , as used for the preparation and measurement of the qutrit.  $R_n^\ell(\phi)$  is a rotation in the qutrit subspace spanned by  $|0\rangle$  and  $|\ell\rangle$  of angle  $\phi$  about axis  $\hat{n}$ . The pulse sequence is applied from right to left.

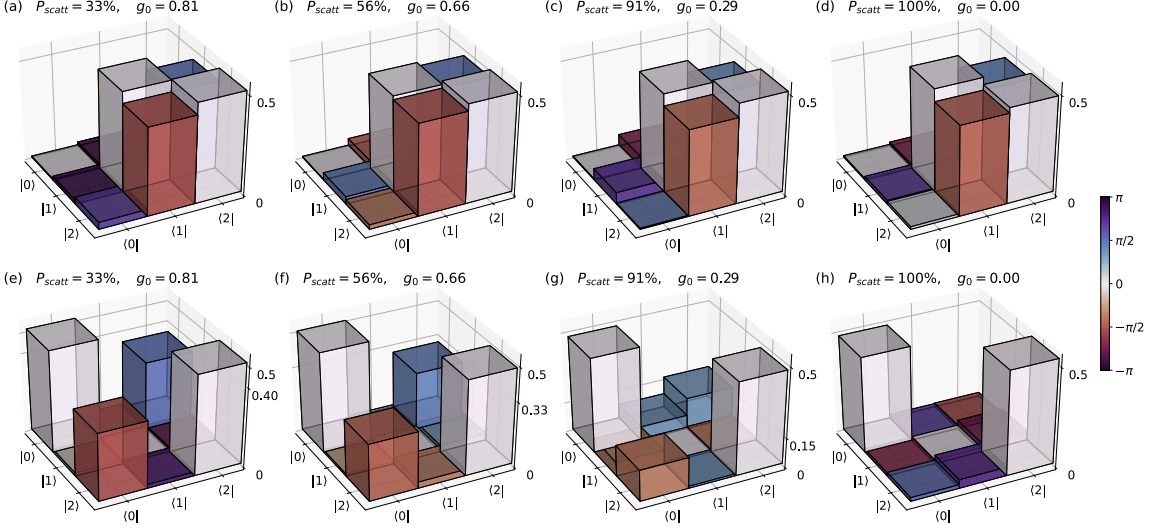


FIG. 3. Reconstructed density matrices  $\rho$  from the experimental data for the initial states  $\frac{1}{\sqrt{2}} (|1\rangle + i|2\rangle)$  [(a) – (d)] and  $\frac{1}{\sqrt{2}} (|0\rangle + i|2\rangle)$  [(e) – (h)]. The colors indicate the complex phase,  $g_0$  is calculated according to our model, see Eq. (7). From (a) to (d) and from (e) to (h) the coupling strength of  $|0\rangle$  to the photon environment is increased and coherences involving state  $|0\rangle$  are destroyed. Thus the off-diagonal elements are preserved from (a) to (d) (state  $\frac{1}{\sqrt{2}} (|1\rangle + i|2\rangle)$ ) while the off-diagonal elements decrease from (e) to (h) (state  $\frac{1}{\sqrt{2}} (|0\rangle + i|2\rangle)$ ).

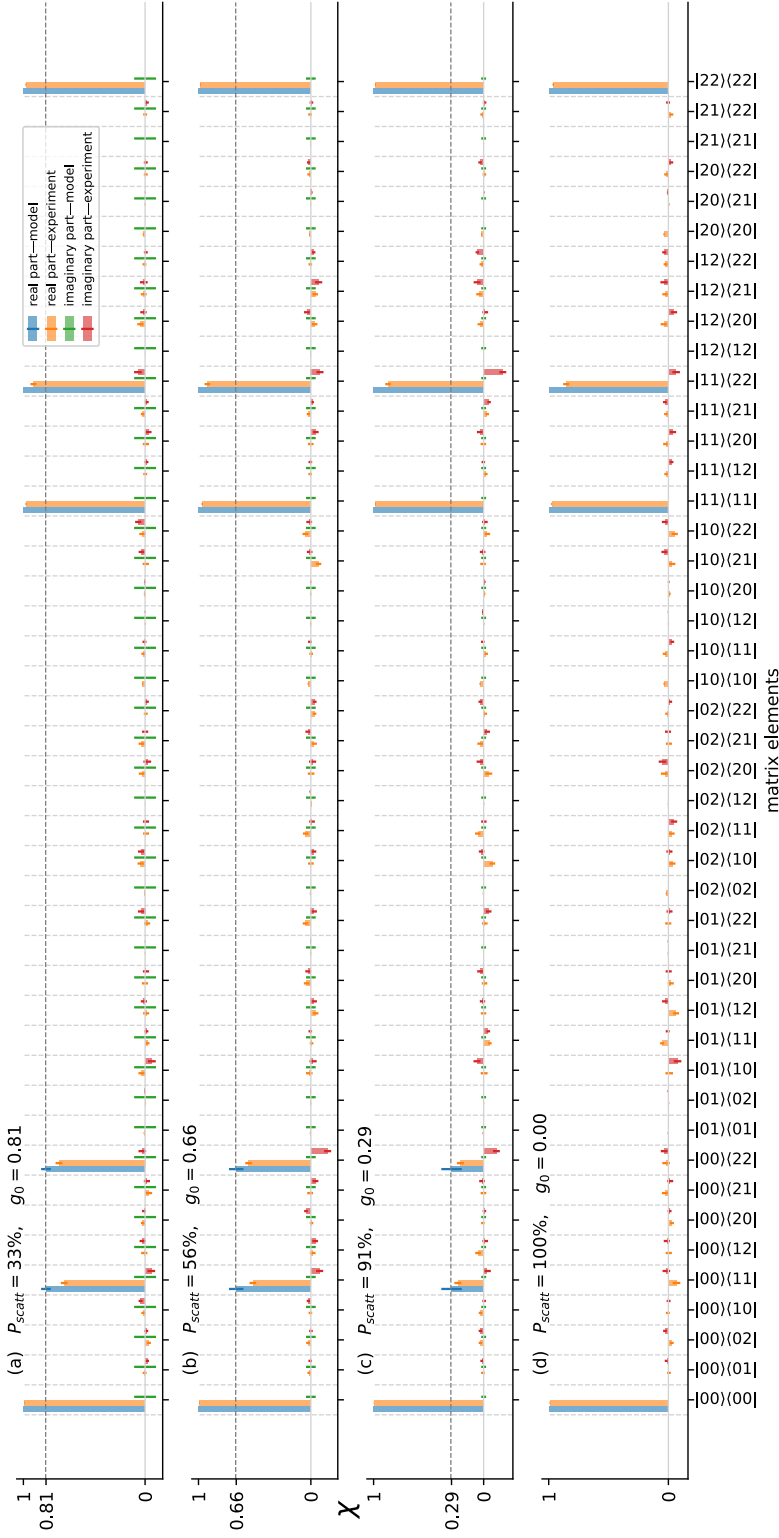


FIG. 4. Comparison of the elements of the experimentally-determined Choi matrices  $\chi_{\text{exp}}$  and model predictions  $\chi_m$ . From (a) to (d) the coupling strength of  $|0\rangle$  to the photon environment is increased (see Appendix Table I) and coherences involving state  $|0\rangle$  are destroyed. (d) is most similar to the ideal Lüders process, from (d)  $\rightarrow$  (a) the process becomes more similar to the trivial process  $\rho \mapsto \rho$ . Error bars in the model result from uncertainties in the experimental parameters  $\Omega$  and  $\Delta$  (68% confidence interval). Error bars in the experimentally-determined Choi matrix elements result from quantum projection noise (68% confidence interval).